TISSUE ENGINEERING: Part A
Volume 18, Numbers 15 and 16, 2012
© Mary Ann Liebert, Inc.
DOI: 10.1089/ten.tea.2012.0079

Engineering Muscle Tissues on Microstructured Polyelectrolyte Multilayer Films

Claire Monge, Ph.D.,[1,*] Kefeng Ren, Ph.D.,[1,*] Kevin Berton, B.S.,[2] Raphael Guillot, M.Sc.,[1] David Peyrade, Ph.D.,[2] and Catherine Picart, Ph.D.[1]

The use of surface coating on biomaterials can render the original substratum with new functionalities that can improve the chemical, physical, and mechanical properties as well as enhance cellular cues such as attachment, proliferation, and differentiation. In this work, we combined biocompatible polydimethylsiloxane (PDMS) with a biomimetic polyelectrolyte multilayer (PEM) film made of poly(L-lysine) and hyaluronic acid (PLL/HA) for skeletal muscle tissue engineering. By microstructuring PDMS in grooves of a different width (5, 10, 30, and 100 μm) and by modulating the stiffness of the (PLL/HA) films, we guided skeletal muscle cell differentiation into myotubes. We found optimal conditions for both the formation of parallel-oriented myotubes and their maturation. Significantly, the myoblasts were collectively prealigned to the grooves before their differentiation. Before fusion, the highest aspect ratio and orientation of nuclei were observed for the 5 and 10 μm wide micropatterns. The formation of myotubes was observed regardless of the size of the micropatterns, and we found that their typical width was 10–12 μm. Their maturation was characterized by the immunolabeling of type II isomyosin. The amount of myosin striation was not affected by the topography, except for the 5 μm wide micropatterns. We highlighted the spatial constraints that led to an important nuclei deformation and further impairment of maturation within the 5 μm grooves. Altogether, our results show that the PEM film combined with PDMS is a powerful tool that is used for skeletal muscle engineering. This work opens perspectives for the development of skeletal muscle tissue in contact with films containing bioactive peptides or growth factors as well as for the study of pathogenic myotubes.

Introduction

Multinucleated myotubes and myofibers are formed by the fusion of mononucleated myoblasts during skeletal muscle development or repair. However, the muscle tissue is not able to self-repair after significant tissue loss due to tumor ablation, injury, congenital defects, or prolonged denervation.[1] *In vitro* tissue engineering represents an alternative for the replacement of damaged tissue, which is a current challenge in regenerative and translational medicine. In order to mimic the physiological architecture of skeletal muscle cells, the development of muscle tissue *in vitro* should be precisely controlled to distribute the critical signals throughout myogenesis. Cell behavior and cell fate are directed by soluble factors (growth factors, cytokines…), biochemical factors (components of the extracellular matrix [ECM]), cell-cell interactions, and the mechanical properties of the substratum in which they are grown. Previous studies have shown the importance of mechanical properties such as stiffness for cell adhesion, spreading, proliferation, and differentiation.[2,3]

One of the main issues of *in vitro* skeletal muscle tissue engineering is to obtain a properly organized tissue. On flat tissue culture polystyrene (TCPS), myotubes are randomly organized, while natural muscle cells are perfectly aligned. This disorganization severely interferes with differentiation studies; notably, synchroneous contraction as the primary function of skeletal muscle is the generation of a longitudinal force.[4] Thus, the controlled alignment of myoblasts and myotubes *in vitro* could have significant application clinically, as it is a crucial step in myofibrillogenesis.[5–8] Furthermore, it has been shown that myoblast adhesion and the subsequent formation of myotubes *in vitro* are sensitive to microstructured topography[9–11] as well as to the biochemical cues presented as micropatterned areas of ECM proteins.[12] Mechanical tension and stretching can also contribute to myoblast alignment, fusion, and maturation.[13,14]

In the present study, we aimed at controlling the alignment of myotubes *in vitro* and at investigating nuclear orientation by combining a microstructured substrate for

[1]LMGP, CNRS UMR 5628 (LMGP), Grenoble Institute of Technology and CNRS, Grenoble Cedex, France.
[2]LTM, CNRS/UJF-Grenoble1/CEA, Grenoble Cedex, France.
*These two authors contributed equally to this work.

guiding cell adhesion and differentiation with a thin film coating with tunable mechanical properties.

To achieve this goal, we used an easy-to-shape biomaterial, polydimethylsiloxane (PDMS). PDMS is a biocompatible[15] and stretchable material that can be easily molded and structured, making it an ideal candidate for both biomedical applications and musculo-skeletal tissue engineering *in vitro*.[16] However, one of the major drawbacks of PDMS is its hydrophobicity, which renders cell cultures over long time periods difficult to maintain. Indeed, the surface modification of PDMS by the adsorption of ECM proteins, such as gelatin,[17] fibronectin,[18] or laminin,[9] by covalent grafting[19,20] or polyelectrolyte multilayer (PEM) coating,[21] is required for long-term cell adhesion. In the present study, we use PEM films as biomimetic matrices with tunable stiffness to modify the PDMS surface. To this end, we have chosen poly(L-lysine) and hyaluronic acid (PLL/HA) films that can be chemically cross-linked and which allow cell culturing over a long time period, as previously shown with regard to myoblasts.[22]

Our strategy was to combine the flexibility of PDMS to achieve surface structuring with the adjustability of the $(PLL/HA)_{12}$ films to fine tune stiffness to support the development of a polarized network of mature myotubes.

Materials and Methods

Reagents

SYLGARD 184 kit (Dow Corning) was used for the fabrication of PDMS. PLL (26 kDa, P2636), FITC-labeled PLL (PLL^{FITC}, P3543) were purchased from Sigma. HA of MW 360 kDa was purchased from Lifecore Biomedical. For film cross-linking, 1-ethyl-3-(3-dimethylamino-propyl)carbodiimide (EDC) and N-hydrosulfosuccinimide (sulfo-NHS) were purchased from Sigma. Cell culture reagents were from Gibco–Invitrogen. Fetal bovine serum (FBS) and horse serum (HS) were purchased from PAA Laboratories. Rhodamine phalloidin (P2141) and the antibodies anti-vinculin (V9131), anti-Troponin T (T6277), and monoclonal anti-skeletal myosin heavy chain (MHC, fast twitch [type II] isomyosin, M4276) were purchased from Sigma. Antibody anti-myogenin was purchased from Tebu-Bio (M225-sc576; Santa Cruz Biotechnology). Alexa Fluor 488-conjugated antibodies, Hoechst 33342, and the Prolong antifade Gold reagent were purchased from Molecular Probes-Invitrogen. All the other reagents were purchased from Sigma and used as received.

Silicon mold and PDMS pattern fabrication

The topographically patterned surface was fabricated by molding PDMS against a silicon mold. First, an SU8 resist layer was spun coated on a silicon substrate and patterned by conventional photolithography. Then, the silicon mold was etched in a high-density plasma chamber with the following gas mixture: $Cl_2/HBr/O_2$.[23] After resist stripping, an OPTOOL layer was wet deposited on the mold as an anti-adhesive layer.[24] For preparation of the PDMS sample with or without patterns, a solution consisting of an elastomer base and a curing agent (10:1 v/v ratio) was thoroughly mixed and placed under a primary vacuum to remove bubbles. 2 mL of the mixture was poured over the silicon mold and cured at 150°C for 10 min. The PDMS sample was then carefully peeled off from the silicon mold and cut into small pieces (10 × 10 mm).

Film preparation and cross-linking procedure

Before the buildup of films, the PDMS substrates were oxidized by oxygen plasma in a microwave downstream etcher (Plassys) at 1500 W power for 10 s. The films were prepared as previously described[25] with an automated dipping machine (Dipping Robot DR3; Kierstein GmbH) on PDMS pieces or on 14 mm-diameter glass slides (VWR Scientific), used here as control substrates. PLL at 0.5 mg/mL, HA at 1 mg/mL, and polyethyleneimine (as precursor layer) at 2 mg/mL were dissolved in an HEPES-NaCl buffer (20 mM HEPES and 0.15 M NaCl at pH 7.4). During $(PLL/HA)_{12}$ film buildup, all the rinsing steps were performed with a rinsing solution (0.15 M NaCl, pH 6.5). After buildup, the films were cross-linked following a previously published protocol[25] using EDC and sulfo-NHS. EDC was used at various concentrations (10, 30, 70, or 100 mg/mL), while sulfo-NHS was kept constant at 11 mg/mL. The films were incubated overnight at 4°C in the cross-linking solution (in 0.15 M NaCl, pH 5.5). Finally, they were rinsed thrice with the HEPES-NaCl buffer.

Micropattern and film characterization

PDMS micropatterns were characterized using an FEI-QUANTA250 scanning electron microscope in a high-vacuum mode. No metallic coating was used to obtain images of the PDMS samples that were deposited on carbon paint. Confocal laser scanning microscopy (CLSM) was used to characterize the PEM films deposited onto the patterns. Confocal images of $(PLL/HA)_{12}$-PLL^{FITC} films were acquired using a Zeiss LSM 700 microscope with an excitation set at 488 nm and an emission set at 505–530 nm.

Cell culture

C2C12 cells (from ATCC; < 20 passages) were maintained in Petri dishes in at 37°C, 5% CO_2, and cultured in a 1:1 Dulbecco's modified Eagle's medium (DMEM)/Ham's F12 medium (growth medium [GM]) supplemented with 10% FBS, containing 10 U/mL penicillin G and 10 μg/mL streptomycin. The cells were subcultured before reaching 60%–70% confluence (approximately every 2 days). For cell culture on the films or TCPS, the cells were seeded at 20,000 cells/cm^2 in GM. For differentiation, the C2C12 cells were allowed to grow for 2 days in GM and then switched to the differentiation medium (DM, 1:1 DMEM/F12) supplemented with 2% HS, containing 10 U/mL penicillin G and 10 μg/mL streptomycin. Phase-contrast images were taken at 4, 24, 48 h, and 3 days using an Axiovert 200M (Zeiss).

Immunofluorescence

For the staining of vinculin, myogenin, troponin T, and skeletal MHC cells were fixed in 3.7% formaldehyde in PBS for 20 min and permeabilized for 4 min in TBS (0.15 M NaCl, 50 mM Tris-HCl, and pH 7.4) containing 0.2% Triton X-100. Samples were blocked in TBS containing 0.1% bovine serum albumin for 1 h, and were then incubated with rabbit anti-myogenin (1:60), mouse anti-skeletal MHC (1:500), mouse anti-vinculin (1:400), or mouse anti-troponin T (1:100)

antibodies in TBS with 0.2% gelatin for 30 min. Alexa-Fluor488-conjugated secondary antibody was then incubated for 30 min. For actin staining, the cells were incubated for 30 min with phalloidin-rhodamine (1:800). The nuclei were stained with Hoechst 33342 at 5 μg/mL for 10 min at room temperature. All the samples were mounted onto coverslips with Prolong antifade reagent and viewed under a fluorescence microscope (Axiovert 200M, Zeiss, Germany or Zeiss LSM 700 for confocal images). Images were acquired with Metaview software using a CoolSNAP EZ CCD camera (both from Ropper Scientific).

Preparation of biological samples for scanning electron microscopy

Cells grown on cross-linked films for 2 days in GM and 3 days in DM were fixed in a solution containing 2% glutaraldehyde, 0.1 M sodium cacodylate, and 0.1 M sucrose (pH 7.2). Samples were then gradually dehydrated using increasing concentrations of ethanol (from 10% to 100%) and left overnight at 37°C. No metallic coating was used. Pictures were taken with an FEI-QUANTA250-SEM-FEG in a high vacuum mode.

Image analysis and statistics

All image quantifications were performed using Image J software v1.43m (NIH). The aspect ratios were determined by dividing the length of nuclei by their width. The degree of orientation of nuclei was manually obtained by determination of the angle formed between the nucleus in the longitudinal way and the edges of the pattern. The labeling of troponin T was used for the analysis of the fusion index (FI) and the alignment of the myotubes. FI was determined by dividing the total number of nuclei in the myotubes (≥ 2 nuclei) by the total number of nuclei counted.[26] The alignment of the myotubes was also manually obtained by determination of the angle formed between the myotubes and patterns. The percentage of striation of the myotubes was determined after the labeling of skeletal MHC and by dividing the number of striated myotubes by the total number of myotubes.

The results represent three independent experiments. More than 100 myotubes and nuclei were analyzed for each condition. Data are reported as mean ± standard error of the mean, and statistical comparisons using SigmaPlot software were performed by All Pairwise Multiple Comparison Procedures (Dunn's Method). Statistically different values are reported in the figures ($p < 0.05$ was considered significant).

Results

Cell adhesion and differentiation on flat PDMS coated by (PLL/HA) film

The first step of the study was to validate the use of PDMS coated with PEM films for long-term myoblast cultures, that is, for a period of time enabling myotube formation and maturation. The myoblasts were seeded onto this substrate hereafter named SilPEM, made of PDMS as an underlying substrate coated by the PEM film $(PLL/HA)_{12}$ with varying stiffness.

Cell adhesion, spreading, and differentiation were investigated for the films of different stiffness that were obtained by increasing the concentration as cross-linker (EDC), as previously shown by our group.[25] The adhesion of C2C12 on stiff films (EDC70, EDC100) was effective, as cells exhibit a characteristic fibroblastic morphology; whereas on softer films (EDC30), cells remain round and exhibit a preference for cell-cell interactions (Supplementary Fig. S1; Supplementary Data are available online at www.liebertpub.com/tea). There was no detachment of the $(PLL/HA)_{12}$ film from PDMS even after 9 days of culture (data not shown). After 2 days in GM when confluency was reached, the medium was switched to DM to induce myogenesis. The formation of myotubes was observed on stiff film after 3 days in DM (Supplementary Fig. S1). After 5 days in DM, the morphology of the myotubes was different depending on the level of cross-linking (Fig. 1A–E). Only a few myotubes were formed on EDC10 films (Fig. 1B). On EDC30 films, myoblast differentiation was poor, even after 5 days in DM (Fig. 1C). For myotubes grown on plastic or stiff films (EDC70 and EDC100), the myotubes were thick and long (Figs. 1A, D, E). Higher magnification and immunolabeling of MHC were used to characterize the development of the myotubes. The FI (Fig. 1F) and the number of striated myotubes (Fig. 1G) were calculated. Striated organization of the cytoskeletal protein MHC is a hallmark of the acquisition of a contractile phenotype by the scaffolding of sarcomeric protein. On the soft EDC10 film, around 13% of myoblasts fused, but the myotubes formed were thinner compared with the myotubes formed on TCPS (Fig. 1B′, F). These myotubes exhibited only around 10% of MHC striations (Fig. 1G). On EDC30 films, the myoblasts did not differentiate and maintained a rounded shape with a very low amount of fusion events (Fig. 1C′). For stiffer EDC70 films, the number of fusion events increased, and the FI reached 15% (Fig. 1F). MHC striations became clearly visible in more than 40% of the myotubes (Fig. 1D′ [inset], G) witnessing the maturity of the myotubes grown on these films. On EDC100 cross-linked films, the FI was higher than on EDC70 films (22% and 15% respectively), but the amount of striated myotubes was twice lower (Fig. 1F, G).

Scanning electron microscopy (SEM) images of myotubes taken after 3 days in DM illustrate the difference in the morphology of myotubes on soft (EDC10) or stiff (EDC70, EDC100) films (Fig. 2A–C). On soft films, the myotubes were rare, often thin, and not well formed. The myotubes were also often egg shaped, resulting from hyperfusion, which explained the high value of FI. On stiff films (Fig. 2B, C), myotubes had a width of $\sim 10\,\mu m$. The optical cross-section of myotubes (Fig. 2D) highlighted their regular cylindrical shape and the alignment of the nuclei. Thus, the stiff $(PLL/HA)_{12}$ films appeared to be more suitable here than the soft films for myotube development.

To investigate whether the sequence of myogenic events was influenced by the underlying substrate, stiff (EDC70) films were built on different materials: PDMS and glass coverslips, which were compared with bare TCPS. The level of the myogenic marker myogenin was determined by immunofluorescence. There was no difference in myogenin levels between PDMS and glass (taken here as control), as shown by the percentage of myogenin-positive cells (Table 1). Thus, ~22%–26% of the cells expressed myogenin after 2 days in DM, independent of the nature of the underlying substrate. Altogether, these results validated PDMS as an

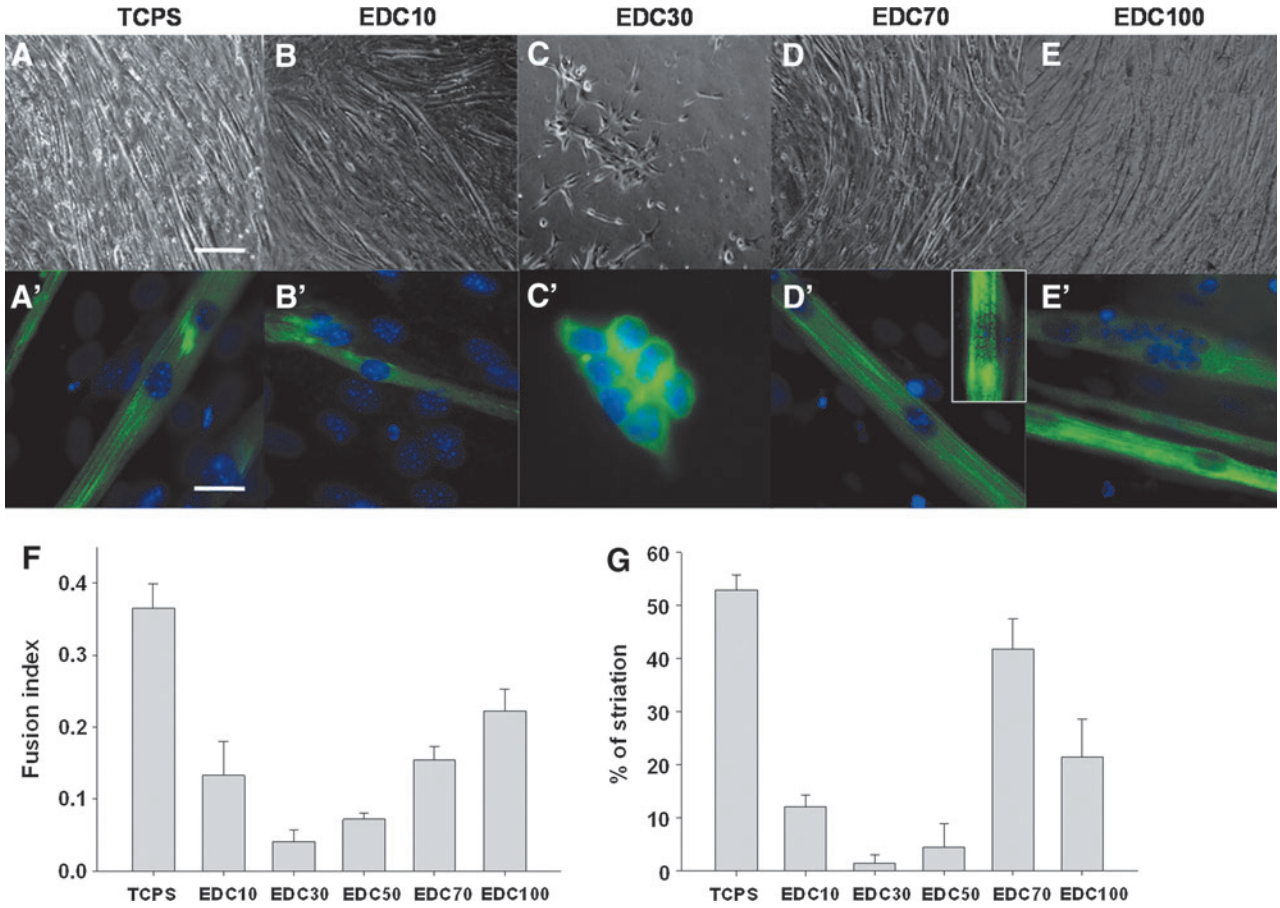

FIG. 1. Differentiation of myoblasts in myotubes as a function of the cross-linking extent of the poly(L-lysine) and hyaluronic acid (PLL/HA) films deposited on flat polydimethylsiloxane (PDMS). Quantification of fusion index (FI) and myosin heavy chain (MHC) striation according to the film cross-linking after 5 days in differentiation medium. Different 1-ethyl-3-(3-dimethylamino-propyl)carbodiimide (EDC) concentrations were used. Tissue culture polystyrene (TCPS) was used as a control. **(A–E)** Phase-contrast microscopy observations of the morphology of myotubes, scale bar 50 μm. **(A′–E′)** Staining of the nuclei (Hoechst) and of MHC, scale bar 10 μm. **(F)** FI. More than 1 000 nuclei were counted for each condition. **(G)** Quantification of MHC striations expressed as a percentage of striated myotubes (more than 50 myotubes analyzed per condition). The experiments were repeated at least thrice, and 5–10 pictures were taken for each condition. Data are represented as mean ± standard error of the mean. Color images available online at www.liebertpub.com/tea

inert substrate for PEM film deposition and subsequent myoblast differentiation in myotubes. SilPEM cross-linked with EDC70 appeared to be the best condition in terms of myotube maturation. Thus, this condition was chosen for all the other experiments.

However, these results on flat surface also draw attention to the stochastic distribution and orientation of myotubes (Fig. 1A and Supplementary Fig. S1; TCPS). The formation of myotubes highly depends on the orientation and motility of myoblasts. On a flat surface, the myoblasts can migrate in all directions. leading to randomly orientated myotubes. In order to align the myotubes in a parallel network as they do *in vivo*, we decided to provide an additional functionality by microstructuring the PDMS substrate.

Characterization of the patterns

Our approach was to linearly orient myoblast fusion to control myotube directionality. Myotubes were shown to be cylindrical. Thus, we chose to create linear grooves in PDMS, as this geometry is close to the shape of a myotube linear with a volume where the myotube may fit in. The grooves were chosen with variable widths to determine the best lateral dimension that has to be given to the single cells to form mature myotubes. The widths were also chosen to be large enough to enclose one or more cells. The PDMS grooves were, thus, formed from a silicon master with different widths: 5, 10, 30, and 100 μm (Fig. 3A). Five and 10 μm are lower than the diameter of a myotube and allowed an investigation of the effect of constriction. Thirty and 100 μm are wider and can be used to study the consequence of lateral spacing for larger patterns. The width of the grooves and of the ridges was equal ($a = b$on Fig. 3B), and the height of the pattern was fixed at 4 μm. This distance was high enough to create a steep change in topography compared with the cell size but small enough to not completely compartmentalize the cells. The deposit of the film built on the microstructured PDMS was observed by using PLL^{FITC} as the final deposited layer.[27] The SilPEM cross-section showed that the film was following the outline of the pattern and had a squared shape

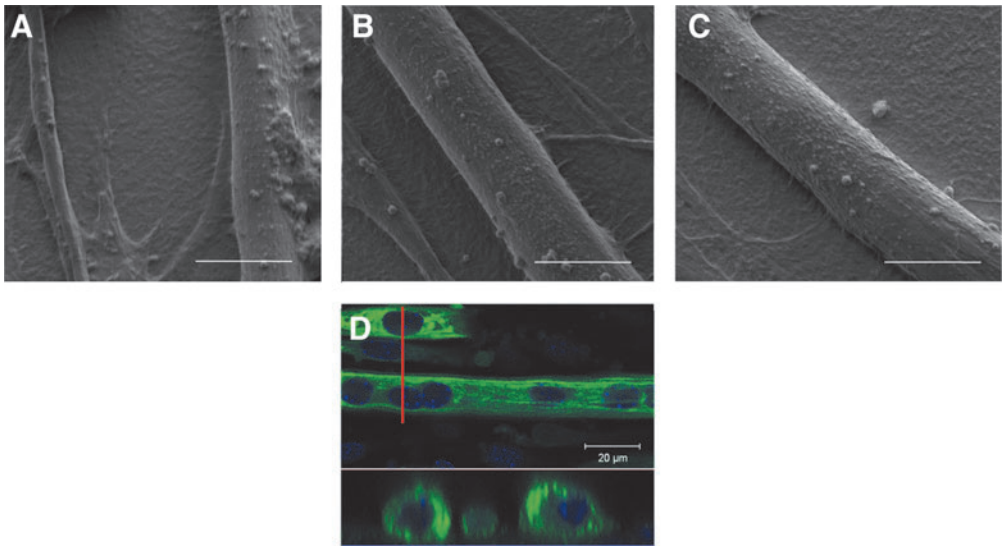

FIG. 2. Scanning electron microscopy (SEM) and confocal laser scanning microscopy (CLSM) images of myotubes formed on cross-linked (PLL/HA) films. **(A–C)** Films were cross-linked with EDC10 **(A)**, EDC70 **(B),** and EDC100 **(C)**. Pictures were taken after 3 days in differentiation medium (DM) and captured at ×4000 magnification, scale bar 30 μm. **(D)** CLSM sections on myotubes grown on EDC70 film for 5 days in DM (MHC in green and nuclei stain by Hoechst in blue). The bottom view represents a cross-section along the red line. Color images available online at www.liebertpub.com/tea

(Fig. 3B). The thickness of the $(PLL/HA)_{12}$ film was ~1 μm, which corresponded well to the previously measured thickness for such films.[28]

Control of cell alignment by microstructured surface

Our strategy was based on the creation of topographic rails for physical guidance. Myoblasts were seeded onto microstructured SilPEM and observed before confluency, at confluency, and after fusion for 5 days in DM.

Early orientation was assessed by determining the orientation of the nuclei in cells plated on patterns after 15 h in GM (Fig. 4). Myoblasts plated on patterns of a width smaller than 30 μm exhibited early parallel orientation and an elongated morphology (Fig. 4A). On 5- and 10 μm-wide patterns, the shape of the nuclei became oval with a median aspect ratio of 1.75 and 1.7, respectively (Fig. 4B, C); on patterns equal to or larger than 30 μm, the cells tended to orient randomly, and cell extensions were arbitrarily directed. On 30–100 μm patterns and on flat surfaces, the nuclei were more circular (aspect ratio <1.5, Fig. 4C). Indeed, the width of the nuclei of myoblasts after 15 h of adhesion increased with the width of the micropatterns from ~8 μm for the thinnest groves to ~13 μm for the largest ones (Fig. 4D). The orientation of the nuclei was also strongly dependent on the width of the patterns (Fig. 4E). On small patterns (5 and 10 μm), the nuclei were almost parallel to the patterns with a tilting angle <10°. On wider patterns, the mean tilting angle progressively increased with the width of the micropatterns. It was <15° for the 30 μm patterns and ~30° for the 100 μm patterns. A wider distribution of orientations was found for the cells on a flat film. The same characteristics were found at 100% confluency (Supplementary Fig. S2) but to a lesser extent due to the cell-cell interactions that maintain the dense cellular network in a given configuration. Thus, the maximum angle reached by the cells was <10° in the 100 μm pattern. It is important to note that overconfluency was never reached to avoid cell detachment as previously reported.[9]

Table 1. Quantification of the Number of Myogenin-Positive C2C12 Myoblasts After 1 or 2 Days in Differentiation Medium

	Day 1	*Day 2*
TCPS	19 ± 1	42 ± 2
EDC70 film on glass	10 ± 3	22 ± 2
EDC70 film on PDMS	6 ± 4	26 ± 4

Results are given as a percentage of positive cells. Data are represented as mean ± standard error of the mean.

PDMS, polydimethylsiloxane; TCPS, tissue culture polystyrene; EDC, 1-ethyl-3-(3-dimethylamino-propyl)carbodiimide.

To explore cell orientation after fusion, the culture medium was switched to DM, and the quantification of myotube orientation was performed after 5 days. A polarized network of myotubes was observed in all sizes of patterns. Furthermore, immunostaining of Troponin T highlighted the orientation of myotubes along the pattern (Fig. 5A). The distribution of angles formed by the myotubes and the patterns was more shifted to the left on small patterns (5 and 10 μm) than on larger ones (30 and 100 μm) (Fig. 5B). The mean orientation angle of the myotubes with regard to the line pattern was 5.8° and 8.2°, respectively, for the 5 and 10 μm wide patterns (dashed red lines in Fig. 5B), indicating that the myotubes formed were either parallel or very close to be parallel to the lines. An increase in the orientation angle was observed on larger grooves (11.6° and 18.2° for the 30 and 100 μm wide patterns, respectively). However, it should be noticed that the network of myotubes still followed a cooperative alignment.

To investigate whether the linear micropatterns have an impact on fusion events, the FIs (Fig. 6A) and the percentage

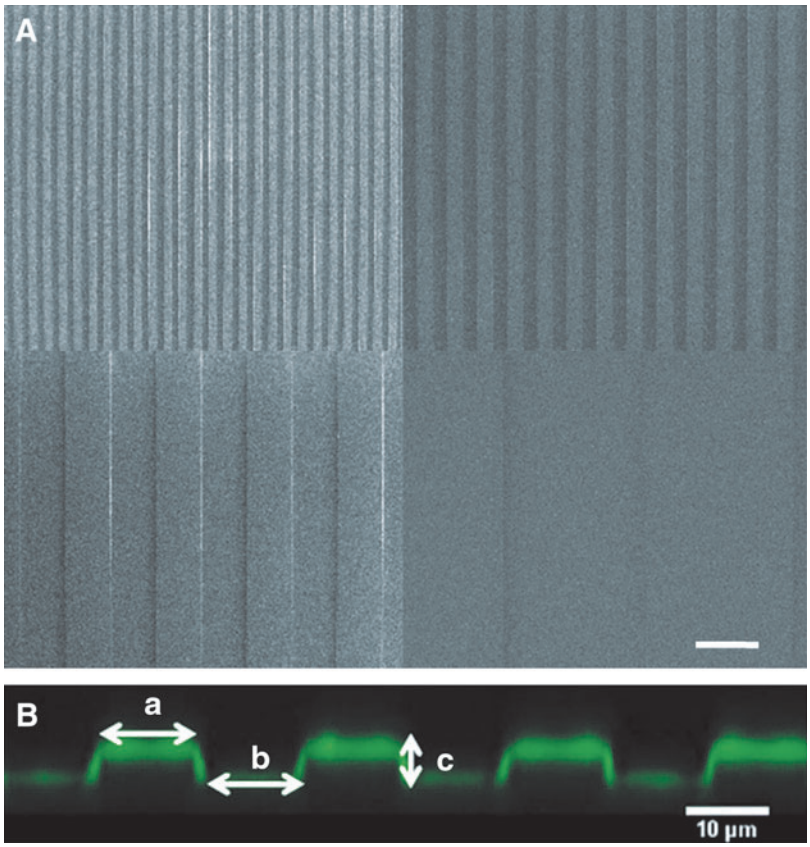

FIG. 3. Characterization of the PDMS micropatterns by SEM and of the film coating by CLSM. **(A)** SEM images of the PDMS mold with the 5, 10, 30, and 100 μm-wide patterns. **(B)** CLSM cross-section of the 10 μm wide micropattern coated by a $(PLL/HA)_{12}$-PLL^{FITC} film. The dimensions *a* and *b* represent the width of the ridge and the groove (*a* = *b*). The dimension *c* represents the height of the pattern. Here, *c* = 4 μm. Color images available online at www.liebertpub.com/tea

of myogenin positive cells on the patterns (Fig. 6B) were determined for the different conditions. No significant difference was found for these two parameters. The maturation state of the myotubes after 5 days in DM was characterized by the % of myotubes exhibiting MHC striations (Fig. 6C). Except for the smallest pattern in which less than 35% of the myotubes were striated, ~50% of the striated myotubes were counted. The 5 μm pattern was statistically different from all the other patterns.

Furthermore, the median width of the myotubes was determined to be ~10–12 μm in all sizes of the patterns (Fig. 7A). This indicated that, for the 5 μm patterns, the myotubes were not entirely embedded in the grooves. Indeed, the mean width of the nuclei was ~5.5 μm for the cells grown on the 5×5 μm pattern but increased to ~6.5 μm for all the other micropatterns (Fig. 7B). This pointed out the importance of geometrical constraints due to the micropatterns, which were particularly revealed in the 5 μm-wide micropattern (Fig. 7C), where the nuclei are often embedded in the groove. It should be noted that the width of the nuclei in differentiated myotubes is significantly smaller than that in myoblasts before fusion (Figs. 7B and 4D, respectively). Indeed, in Figure 7C, confocal observations of the nuclei in myotubes adjacent to non-fused myoblasts revealed that the nucleus in non-fused cells is rather flat (11 μm wide and 5 μm high); whereas the nuclei in myotubes are thinner and higher (7 μm wide and 7 μm high). In 10 μm or less patterns, the nuclei of differentiated or non-differentiated cells either adjusted to the width of the groove or the ridge, or straddled the pattern (Fig. 7D for the 10 μm pattern). In patterns wider than 30 μm, the nuclei could straddle likewise, although several nuclei can fit into a groove (Fig. 7D′).

Discussion

Myoblast differentiation is favored in stiff $(PLL/HA)_{12}$ films

The development of muscle tissue *in vitro* requires a combination of signals that converge on the cell. The adhesion of cells to a surface generates a large number of messages determining cell behavior. It is now well established that the regulation of myogenic signals is done through not only cell-cell contact but also cell-matrix interaction.[29,30] Stiffness of the substrate is also recognized as being one of the signals that can influence adhesion and differentiation.[2,31] To create a biomaterial that is able to drive muscle precursor cells toward myofibrillogenesis, the appropriate stiffness has to be found. Due to their tunable mechanical properties, biocompatible PEM films made from PLL and HA can be employed as a coating of biocompatible materials that cannot, in their native form, control cell function. Proper alignment of myotubes is needed for the establishment of *in vitro* models of muscle tissue regeneration. Here, we aimed at combining $(PLL/HA)_{12}$ films with molded PDMS to reproduce *in vitro* the natural organization of myotubes in a regular and parallel network. Being a biocompatible material, PDMS is a good candidate for biomedical applications. However, due to its hydrophobic properties, bare PDMS is not suitable as a substrate for persistent C2C12 culture, as cells detached after 48 h in GM (Supplementary Fig. S1). Earlier, it was shown that the functionalization of PDMS is needed to support the adhesion

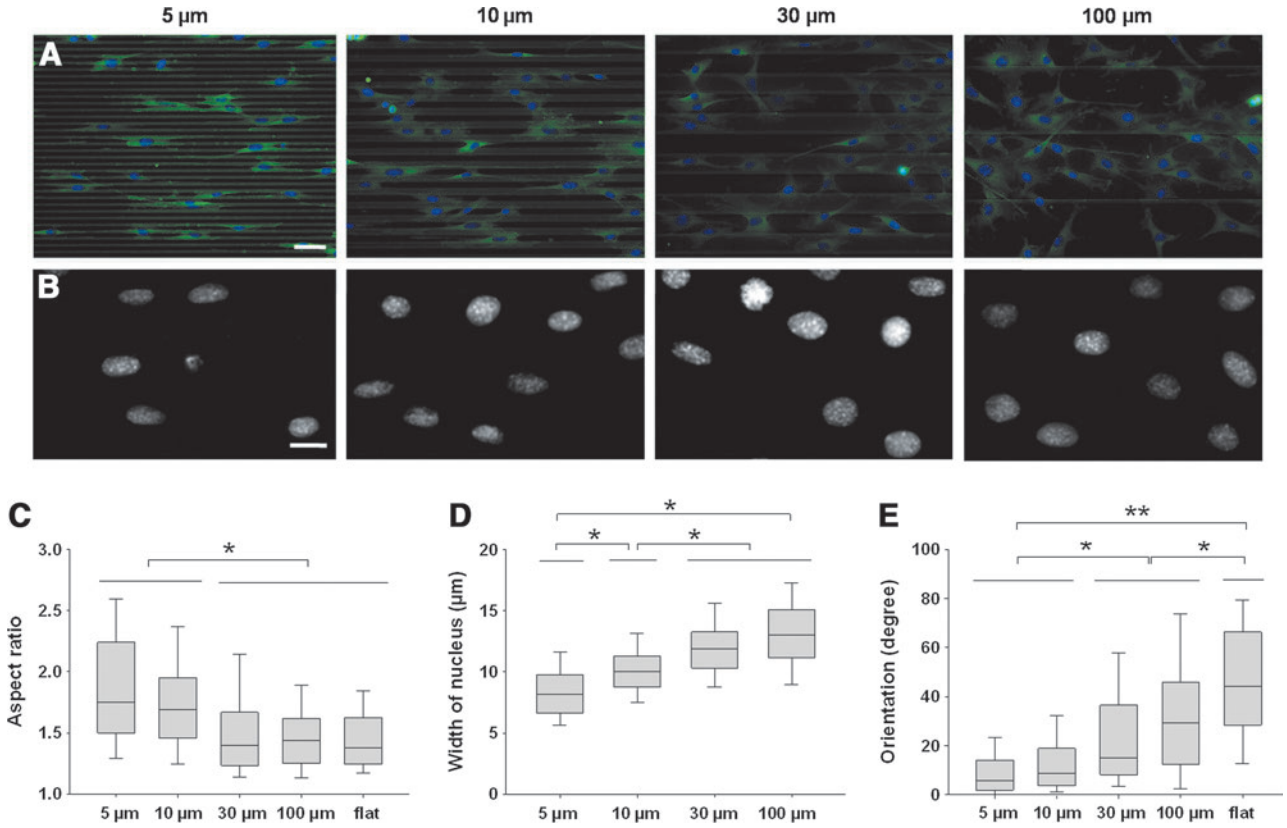

FIG. 4. Early orientation of myoblasts after 15 h of culture in growth medium (GM) on the micropatterns. **(A)** Nuclei staining (Hoechst) and vinculin immunostaining of cells grown out of the micropatterns of increasing width, scale bar 50 µm. **(B)** Magnification of the nuclei of myoblasts on micropatterns, scale bar 20 µm. **(C)** Aspect ratio of nuclei (length over width of the equivalent ellipse) as a function of the width of the micropatterns. **(D)** Width of the nuclei. **(E)** Orientation of nuclei with regard to the main axis of the micropatterns (*$p < 0.05$, **$p < 0.001$). Color images available online at www.liebertpub.com/tea

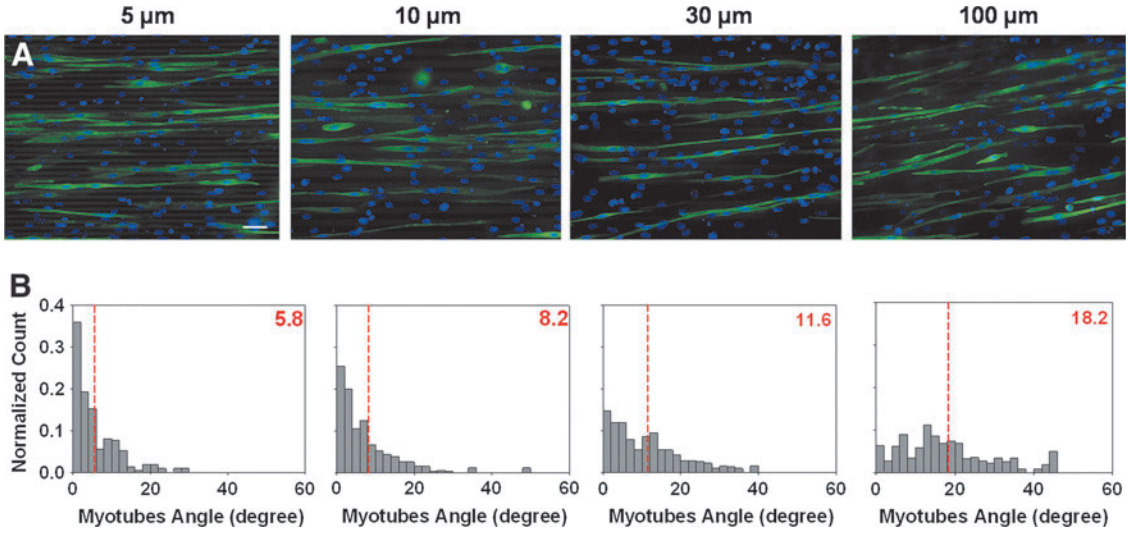

FIG. 5. Influence of polyelectrolyte multilayer (PEM)-coated micropatterns on myotube orientation after 5 days in differentiation medium. **(A)** Troponin T immunostaining and nuclear staining (Hoechst) highlighting the influence of the topography on myotubes alignment, scale bar 50 µm. **(B)** Angle distribution as a function of pattern width. Dashed red lines and values in red represent mean values for four independent experiments in 200–300 myotubes. Color images available online at www.liebertpub.com/tea

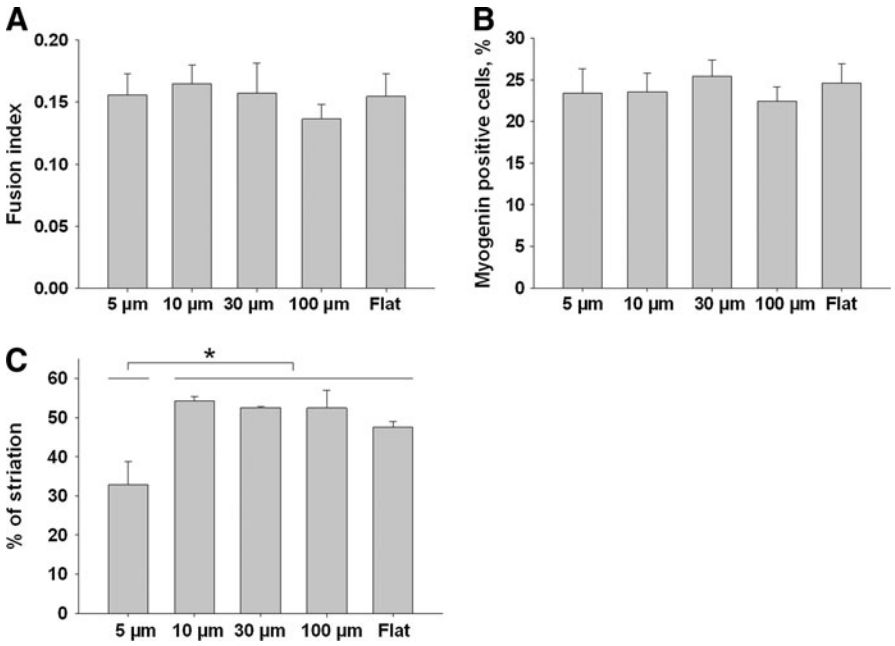

FIG. 6. Characterization of myotube development on the PEM-coated PDMS micropatterns. FI **(A)**, percentage of myogenin-positive cells **(B)** and % of MHC striations **(C)** of myotubes grown 5 days in differentiation medium on the various widths of grooves (5, 10, 30, 100 µm, or flat surface). Data are represented as mean ± standard error of the mean (*$p < 0.05$).

and proliferation of various cell types, including fibroblasts[19] and vascular smooth muscle cells.[32] For C2C12 cells, previous studies used PDMS in combination with a coating of an ECM protein, either laminin[9,11] or collagen.[33] However, batch-to-batch quality of the protein and initial state of the PDMS substrate may lead to poor reproducibility in the results between different research groups.

It was only recently that the potential of PEM films as a PDMS coating has been explored both for mammalian cells[21] and for yeast.[34] However, to the best of our knowledge, no study has explored the combination of PDMS microstructuration and PEM coating that provides a substrate for muscle differentiation over a long time period (typically a week) for muscle tissue engineering. The deposit of a (PLL/

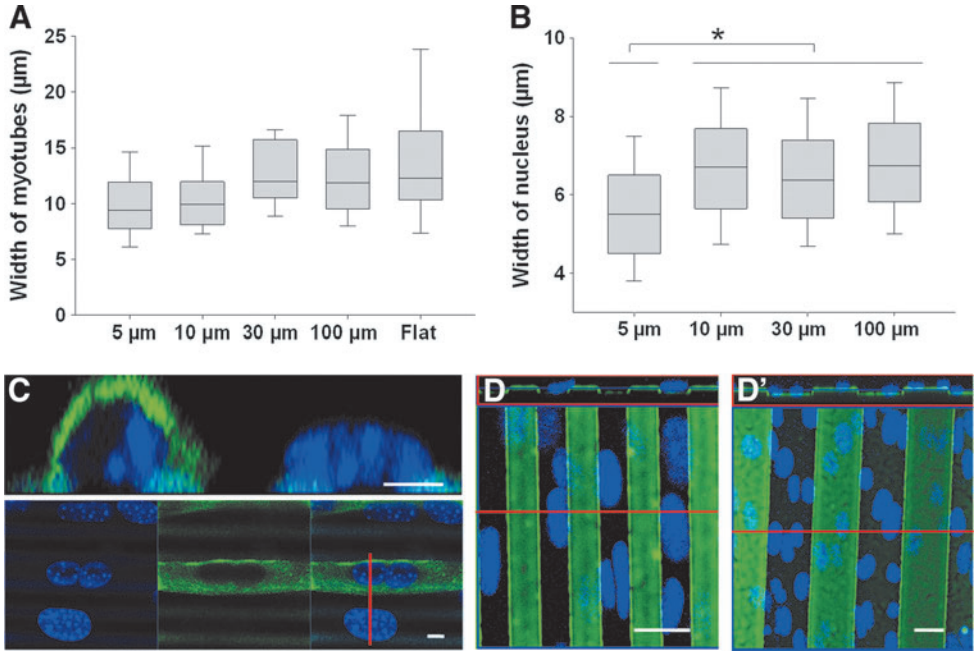

FIG. 7. Characterization of the width of the myotubes and the nuclei of the myotubes on the PEM-coated PDMS micropatterns. Width of the myotubes **(A)** and of the nuclei of myotubes **(B)** determined on the various widths of grooves (5, 10, 30, and 100 µm). **(C)** Confocal picture and cross-section of a myotube and a myoblast seeded on a 5 µm pattern. Nuclei (Hoechst) and MHC were stained. The red line corresponds to the cross-section line. Scale bar 5 µm. **(D, D′)** Confocal picture and cross-section of cells stained with Hoechst and seeded on 10 µm **(D)** and 30 µm **(D′)** patterns. The PEM films on patterns were labeled with PLL^{FITC}. Scale bar 20 µm. The red line corresponds to the cross-section line. All the pictures were taken after 5 days in differentiation medium (*$p < 0.05$). Color images available online at www.liebertpub.com/tea

$HA)_{12}$ PEM film on PDMS allowed to combine geometrical cues with the versatility of the PEM film coating.

First, we investigated the adequate conditions for myoblast development on flat SilPEM. The mechanical properties of the $(PLL/HA)_{12}$ films were modified by chemical cross-linking[25] and myoblast adhesion, spreading, proliferation, and differentiation were examined. Young's modulus of the films can be varied between several tens of kPa to about 400 kPa depending on the concentration of the cross-linker,[22] which is much softer than glass ($\sim$50 GPa). Indeed, we have previously shown that the stiffness of $(PLL/HA)_{12}$ films built on glass coverslips influenced cell behavior.[22] Soft EDC30 films were not well suited for myoblast culture. Cells were round and tended to cluster instead of spread. Myoblast proliferation was favored in stiffer films (EDC50, 70 and 100) (Supplementary Fig. S1) as well as myotube formation and maturation exhibited the same characteristic (Fig. 1). On EDC70 films, the FI significantly increased when the films were stiffer. Even though the FI for cells grown on PEM films was lower than that on TCPS, $\sim$15% of cells effectively differentiated on EDC70 films.

A surprising outcome was found in EDC10 films that are softer than the EDC30 films but displayed myotube formation with a FI comparable to the value determined in EDC70. This observation of a non-linear response of cell development as a function of substratum stiffness was previously reported in normal myotubes[31] and also in dystrophic myotubes formed on hydrogel by increasing the amount of polyacrylamide.[35] However, in spite of a rather high FI on EDC10, only $\sim$10% of myotubes revealed MHC striations, compared with 40% on EDC70 films. Likewise, the amount of striated myotubes decreased in EDC100 films compared with EDC70 films in spite of a higher FI for EDC70 films. Notably, even if myoblast fusion is a prerequisite for myotube formation, this does not ensure normal myotube development and maturation. The FI should then be carefully considered, and a high FI is not a guarantee of the maturation of the myotubes. On EDC70 films, both the FI and the amount of striated cells were high, which led us to select this condition as the best candidate to favor the development of mature myotubes.

On this flat surface, the average diameter of myotubes determined by SEM and immunofluorescence was $\sim$10 μm (Figs. 2B, D and 7A), with the myotubes having a cylindrical shape. As typically observed for the culture of myotubes on flat surfaces, the global orientation of myotubes was random. In order to limit stochasticity and organize the development of myotubes in a predictable parallel network, we molded the underlying PDMS onto which the $(PLL/HA)_{12}$ film was deposited. This offered the possibility to combine the properties of the PEM film with topography.

Microstructured $(PLL/HA)_{12}$ films lead to parallel alignment of myotubes

Topography and chemistry are two major strategies that are commonly employed to guide myoblast differentiation. The chemical approach consists of micropatterning adhesive areas, typically 50–100 μm wide, that are separated by non-adhesive cell areas of the same distance. The width of the adhesive part should be sufficiently wide (few tens of μm) to allow lateral contact and subsequent fusion events between the myoblasts. For instance, fibronectin was deposited by microcontact printing on TCPS,[12] or parallel lanes of ECM proteins were formed on a polyacrylamide hydrogel.[31,35] This allowed the formation of collectively aligned myotubes.

Topography can be provided by molding the underlying substrate used to culture myoblasts. In this case, the myoblasts can adhere everywhere on the material but position themselves by "contact guidance," as already widely demonstrated for fibroblasts.[36,37] To grow myotubes in 3D, synthetic and natural polymeric materials have been molded into fibers, such as polypropylene,[38] PLLA,[39] or collagen[40] fibers. Etched materials have also been used to create topography: ultrafine grooves on quartz[41] or microgrooves of hydroxyapatite,[42] but cell differentiation may depend on the size (width, depth) of the microstructures. PDMS appears particularly interesting, as it is transparent and easily moldable. However, studies involving microstructured PDMS used an ECM coating such as collagen, fibronectin, or laminin.[11,33,43] However, the adsorption of these proteins on PDMS is very difficult to control and is instable over time.[19] All these studies led to a collective alignment of myotubes, with an angle that depended on the geometry of the micropattern (lines or square patterns). The depth of the pattern was also found to affect myotube alignment,[44,45] with a depth of 2–4 μm leading to a better alignment.

To our knowledge, maturation of the myotubes on microgroved substrates has barely been studied. Maturation, as characterized by myosin striation, is known to depend on the stiffness of the substrate, as shown on patterned polyacrylamide hydrogels,[31,46] and the alignment of myotubes is not necessarily correlated with myosin striation. Indeed, Altomare *et al.* observed a collective alignment on a stiff copolymer of poly(L-lactide acid) and trimethylene carbonate copolymer without the appearance of myosin striation.[44]

The deposits of LbL films that are made of synthetic or natural polymers have recently appeared as an interesting strategy that is used to promote cell attachment on PDMS.[32,47] In our study, a parallel orientation of myoblasts and myotubes was obtained with microstructured SilPEM. We showed here that myoblasts already began to orient and to develop cell extensions following the linear orientation of the pattern after $\sim$15 h in GM (Fig. 4). Thus, the myoblasts were prealigned before fusion. In all micropatterns, the myotubes formed and followed a collective orientation (Fig. 5). They were aligned at an angle $<10°$ on the 5 and 10 μm-wide micropatterns. Of note, even on the widest grooves of 100 μm, where the angle of alignment of myotubes was tilted with regard to the pattern edges, the myotubes were still parallel to each other. Previous studies on cells seeded on linear patterns reported the tilting of myotubes within 20° on 50[33] and 80 μm-wide line patterns.[12,33]

The topography did not inhibit cell fusion

There are only scarce data in the literature on the width of myotubes, which is estimated at $\sim$10–15 μm.[48] The widths of micropatterns were chosen to be lower (5 and 10 μm) and higher (30 and 100 μm) than this typical width. Interestingly, we noted from the micropatterns that the widths of the myotubes were found to be always $\sim$10–12 μm regardless of the size of the micropatterns (Fig. 7A), as if this parameter was solely controlled by a self-organization process.[48]

Nevertheless, the FI was not affected by the myoblasts in microstructured SilPEM, indicating that topography did not influence the total amount of cells fusing.

Two hypotheses may be proposed that explain the formation of multi-nucleated myotubes, which results from the fusion of myoblast with myoblast, myoblast with myotube, and myotube with myotube.[49] The first one is that the cells were not able to migrate between grooves. The presence of a physical barrier induced directionality in the migration. As the cells tended to elongate in the direction of the pattern without any changes in FIs (Figs. 4A and 6A), end-to-end fusion would then probably be favored to provide the myotubes with new cells.[41] The second hypothesis is that cells can overcome the topography and step over a groove of 4 μm in height. Myoblasts and myotubes would, thus, be able to maintain a normal fusion rate and regular muscle morphogenesis in the presence of a 4 μm-high topography. This may be explained by the fact that the 4 μm height of the grooves was smaller than the height of a myotube (~10 μm), leading to exposure of the top of the myotubes outside of the groove. Lateral fusion with cells on the ridge could then occur. The possible restriction of cell migration and the presence (or absence) of lateral fusion onto microstructured SilPEM during myogenesis are questions that will be investigated in future studies.

Intracellular re-organization during myotube development is restricted by thin grooves

Since a width of 5 μm was thinner than the width of a myotube and of the nucleus, this pattern was expected to restrict lateral cell extension and to create spatial constraints. The FI was equal to that on larger grooves, though we observed a significant decrease in the amount of striated myotubes (Fig. 6C). This witnesses the need for a minimum lateral spacing for myotube maturation.

During myogenesis, the cytoskeleton is re-organized during muscle growth,[48] and this may be altered by the presence of the microstructures that create physical obstacles to spreading. There is now growing evidence that there is a

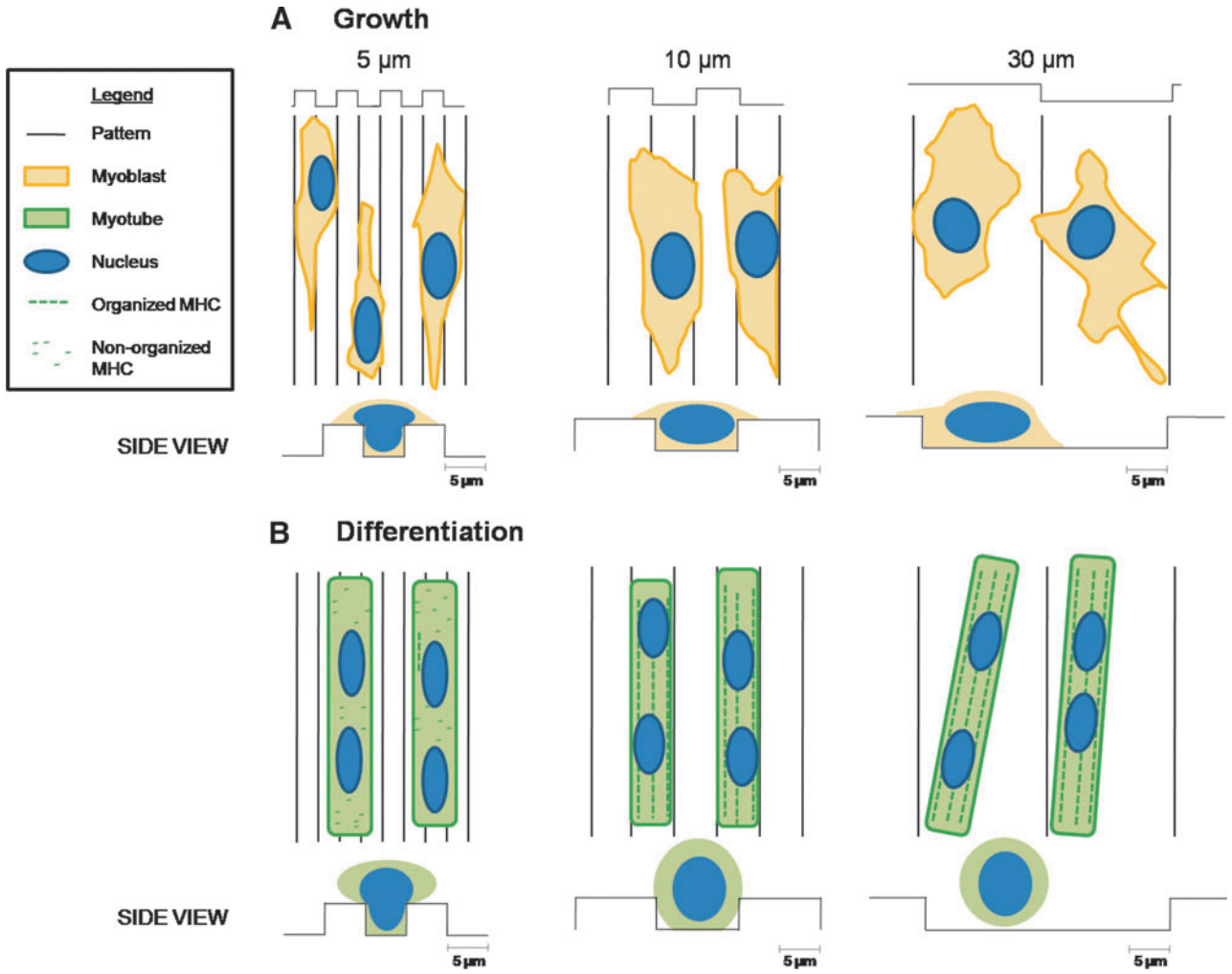

FIG. 8. Myoblast spreading and differentiation on microstructured PDMS coated with PEM film. **(A)** Myoblasts spreading after 24 h in GM. The cytoplasm of the cells spread on the substrate, whereas the nuclei can be confined and deformed by the topography (5 and 10 μm grooves). **(B)** After 5 days in differentiation medium, aligned myotubes are formed in all the patterns, but they only present myosin striation in patterns of 10 um or more. In the 5 μm pattern, the MHC is not organized into sarcomeric architecture, probably because the nuclei structure is confined by the topography. Color images available online at www.liebertpub.com/tea

physical communication (force transmission) between the cytoskeleton and the nucleus through actin-nesprins coupling and possibly other proteins.[50] Nesprins bind to SUN proteins that interact with nuclear lamins via a LINC complex (linker of nucleoskeleton and cytoskeleton), forming stable nuclear structures that can bind DNA. This allows a coupling between the nuclear compartment and the cytoplasm. This nuclear cytoskeletal force transmission is essential for normal cell functioning. For example, a mutation in Nesprin 1 is involved in the pathogenesis of Emery-Dreifuss muscular dystrophy.[51,52] It was recently shown on C2C12 that the interference or disruption of the LINC complex perturbs the mechanical control of cell differentiation.[53] Nucleus positioning is indeed known to be particularly important for the maturation of myofibers: Nuclei from fused cells migrate and modify the shape of the myotubes during myogenesis. In immature myofibers, the nuclei gather at the cell center; whereas in mature myofibers, the nuclei are positioned at the periphery of the cell with clusters at the neuromuscular synapse at advanced development.[54]

The deformation of cell nuclei and of cells in the 5 μm-wide patterns, with a nucleus width of 5.5 μm (Fig. 7B) and a myotube width of less than 10 μm (Fig. 7A), could impair the force transmission via the nucleus. Thus, we hypothesized that the spatial restriction (below myotube diameter) inhibited the normal maturation of myotubes and sarcomer formation by constraining the spreading of the nucleus (Fig. 8).

Possible biomedical applications of SilPEM

A combination of the biocompatible PDMS and a biomimetic $(PLL/HA)_{12}$ film led to a biomaterial with adjustable properties that may be used for medical applications. The substrate can serve as an inductive template for *in vivo* muscle tissue regeneration. The role of the substrate would then be to drive the development, alignment, and further fusion of cells after implantation. For the *in vitro* generation of functional skeletal muscle tissue, coculturing of myoblasts with additional cells would be required: endothelial cells for oxygen and nutrient supply and fibroblasts to stabilize the construct. This tri-culture was first archived successfully by Levenberg *et al.* on a polymer scaffold and is now used as skeletal muscle grafts.[55,56]

As a conclusion, the SilPEM offers a wide range of possibilities, thanks to the versatility of the PEM coating and the molding of PDMS into different shapes. The SilPEM could either serve as a reservoir for delivering bioactive molecules via the PLL/HA films[57] or be grafted with adhesion peptides[58] for possible therapeutic applications in skeletal muscle tissue repair. It could also be used for the triggered release of bioactive molecules by stretching it.[59] Furthermore, the SilPEM may also be employed for mechanistic studies conducted on the maturation of pathological myotubes.

Acknowledgments

C.P. wishes to thank the European Commission for the support rendered via an ERC Starting grant 2010 (GA 259370) and the Institut Universitaire de France for financial support. K.R. is indebted to the Association Recherche contre le Cancer for a post-doctoral fellowship. This work was supported by a BQR 2010 (BQR0592020) from the Grenoble Institute of Technology to C.P. and D.P.

Disclosure Statement

No competing financial interests exist.

References

1. Rossi, C.A., Pozzobon, M., and De Coppi, P. Advances in musculoskeletal tissue engineering Moving towards therapy. Organogenesis **6,** 167, 2010.
2. Engler, A.J., Sen, S., Sweeney, H.L., and Discher, D.E. Matrix elasticity directs stem cell lineage specification. Cell **126,** 677, 2006.
3. Gilbert, P.M., Havenstrite, K.L., Magnusson, K.E.G., Sacco, A., Leonardi, N.A., Kraft, P., *et al.* Substrate elasticity regulates skeletal muscle stem cell self-renewal in culture. Science **329,** 1078, 2010.
4. Stern-Straeter, J., Riedel, F., Bran, G., Hormann, K., and Goessler, U.R. Advances in skeletal muscle tissue engineering. In Vivo **21,** 435, 2007.
5. Wakelam, M.J.O. The fusion of myoblasts. Biochem J **228,** 1, 1985.
6. Bian, W.N., and Bursac, N. Engineered skeletal muscle tissue networks with controllable architecture. Biomaterials **30,** 1401, 2009.
7. Rochlin, K., Yu, S., Roy, S., and Baylies, M.K. Myoblast fusion: when it takes more to make one. Dev Biol **341,** 66, 2010.
8. Knudsen, K.A., and Horwitz, A.F. Toward a mechanism of myoblast fusion. Prog Clin Biol Res **23,** 563, 1978.
9. Lam, M.T., Sim, S., Zhu, X., and Takayama, S. The effect of continuous wavy micropatterns on silicone substrates on the alignment of skeletal muscle myoblasts and myotubes. Biomaterials **27,** 4340, 2006.
10. Charest, J.L., Garcia, A.J., and King, W.P. Myoblast alignment and differentiation on cell culture substrates with microscale topography and model chemistries. Biomaterials **28,** 2202, 2007.
11. Gingras, J., Rioux, R.M., Cuvelier, D., Geisse, N.A., Lichtman, J.W., Whitesides, G.M., *et al.* Controlling the orientation and synaptic differentiation of myotubes with micropatterned substrates. Biophys J **97,** 2771, 2009.
12. Bajaj, P., Reddy, B., Millet, L., Wei, C.N., Zorlutuna, P., Bao, G., *et al.* Patterning the differentiation of C2C12 skeletal myoblasts. Integr Biol **3,** 897, 2011.
13. Kamotani, Y., Bersano-Begey, T., Kato, N., Tung, Y.C., Huh, D., Song, J.W., *et al.* Individually programmable cell stretching microwell arrays actuated by a Braille display. Biomaterials **29,** 2646, 2008.
14. Nakai, N., Kawano, F., Oke, Y., Nomura, S., Ohira, T., Fujita, R., *et al.* Mechanical stretch activates signaling events for protein translation initiation and elongation in C2C12 myoblasts. Mol Cells **30,** 513, 2010.
15. Andriot, M., Chao, S.H., Colas, A., Cray, S., de Buyl, F., DeGroot, J.V., Dupont, A, Easton, A., Garaud, J.L., Gerlach, E., Gubbels, F., Jungk, M., Leadley, S., Lecomte, J.P., Lenoble, B., Meeks, R., Mountney, A., Shearer, G., Stassen, S., Stevens, C., Thomas, X., and Wolf, A.T. Silicone in industrial application. In: De Jaeger, R., and Gleria, M., eds. Inorganic Polymers. New York: Nova Science Publishers, 2007, p. 61.
16. Dennis, R.G., and Kosnik, P.E. Excitability and isometric contractile properties of mammalian skeletal muscle constructs engineered *in vitro*. In Vitro Cell Dev Biol Anim **36,** 327, 2000.

17. Yim, E.K.F., Darling, E.M., Kulangara, K., Guilak, F., and Leong, K.W. Nanotopography-induced changes in focal adhesions, cytoskeletal organization, and mechanical properties of human mesenchymal stem cells. Biomaterials **31,** 1299, 2010.
18. Peterson, E.T.K., and Papautsky, I. Microtextured polydimethylsiloxane substrates for culturing mesenchymal stem cells. Methods Mol Biol **321,** 179, 2006.
19. Wipff, P.J., Majd, H., Acharya, C., Buscemi, L., Meister, J.J., and Hinz, B. The covalent attachment of adhesion molecules to silicone membranes for cell stretching applications. Biomaterials **30,** 1781, 2009.
20. Mikhail, A.S., Ranger, J.J., Liu, L.H., Longenecker, R., Thompson, D.B., Sheardown, H.D., *et al.* Rapid and efficient assembly of functional silicone surfaces protected by PEG: cell adhesion to peptide-modified PDMS. J Biomater Sci Polym Ed **21,** 821, 2010.
21. Kidambi, S., Udpa, N., Schroeder, S.A., Findlan, R., Lee, I., and Chan, C. Cell adhesion on polyelectrolyte multilayer coated polydimethylsiloxane surfaces with varying topographies. Tissue Eng **13,** 2105, 2007.
22. Ren, K., Crouzier, T., Roy, C., and Picart, C. Polyelectrolyte multilayer films of controlled stiffness modulate myoblast cell differentiation. Adv Funct Mater **18,** 1378, 2008.
23. Lalouat, L., Cluzel, B., de Fornel, F., Velha, P., Lalanne, P., Peyrade, D., *et al.* Subwavelength imaging of light confinement in high-Q/small-V photonic crystal nanocavity. Appl Phys Lett **92,** 111111, 2008.
24. Tallal, J., Berton, K., Gordon, M., and Peyrade, D. 4 Inch lift-off process by trilayer nanoimprint lithography. J Vacuum Sci Technol B **23,** 2914, 2005.
25. Schneider, A., Francius, G., Obeid, R., Schwinte, P., Hemmerle, J., Frisch, B., *et al.* Polyelectrolyte multilayers with a tunable Young's modulus: influence of film stiffness on cell adhesion. Langmuir **22,** 1193, 2006.
26. Charrasse, S., Comunale, F., Fortier, M., Portales-Casamar, E., Debant, A., and Gauthier-Rouviere, C. M-cadherin activates Rac1 GTPase through the Rho-GEF trio during myoblast fusion. Mol Biol Cell **18,** 1734, 2007.
27. Picart, C., Mutterer, J., Richert, L., Luo, Y., Prestwich, G.D., Schaaf, P., *et al.* Molecular basis for the explanation of the exponential growth of polyelectrolyte multilayers. Proc Natl Acad Sci U S A **99,** 12531, 2002.
28. Picart, C., Lavalle, P., Hubert, P., Cuisinier, F.J.G., Decher, G., Schaaf, P., *et al.* Buildup mechanism for poly(L-lysine)/hyaluronic acid films onto a solid surface. Langmuir **17,** 7414, 2001.
29. Krauss, R.S. Regulation of promyogenic signal transduction by cell-cell contact and adhesion. Exp Cell Res **316,** 3042, 2010.
30. Buck, C.A., and Horwitz, A.F. Cell-surface receptors for extracellular-matrix molecules. Annu Rev Cell Biol **3,** 179, 1987.
31. Engler, A.J., Griffin, M.A., Sen, S., Bonnetnann, C.G., Sweeney, H.L., and Discher, D.E. Myotubes differentiate optimally on substrates with tissue-like stiffness: pathological implications for soft or stiff microenvironments. J Cell Biol **166,** 877, 2004.
32. Brown, X.Q., Ookawa, K., and Wong, J.Y. Evaluation of polydimethylsiloxane scaffolds with physiologically-relevant elastic moduli: interplay of substrate mechanics and surface chemistry effects on vascular smooth muscle cell response. Biomaterials **26,** 3123, 2005.
33. Huang, N.F., Lee, R.J., and Li, S. Engineering of aligned skeletal muscle by micropatterning. Am J Transl Res **2,** 43, 2010.
34. Schmolke, H., Demming, S., Edlich, A., Magdanz, V., Buttgenbach, S., Franco-Lara, E., *et al.* Polyelectrolyte multilayer surface functionalization of poly(dimethylsiloxane) (PDMS) for reduction of yeast cell adhesion in microfluidic devices. Biomicrofluidics **4,** 44113, 2010.
35. Serena, E., Zatti, S., Reghelin, E., Pasut, A., Cimetta, E., and Elvassore, N. Soft substrates drive optimal differentiation of human healthy and dystrophic myotubes. Integr Biol **2,** 193, 2010.
36. Dalby, M.J., Riehle, M.O., Yarwood, S.J., Wilkinson, C.D.W., and Curtis, A.S.G. Nucleus alignment and cell signaling in fibroblasts: response to a micro-grooved topography. Exp Cell Res **284,** 274, 2003.
37. Berry, C.C., Campbell, G., Spadiccino, A., Robertson, M., and Curtis, A.S.G. The influence of microscale topography on fibroblast attachment and motility. Biomaterials **25,** 5781, 2004.
38. Neumann, T., Hauschka, S.D., and Sanders, J.E. Tissue engineering of skeletal muscle using polymer fiber arrays. Tissue Eng **9,** 995, 2003.
39. Huang, N.F., Patel, S., Thakar, R.G., Wu, J., Hsiao, B.S., Chu, B., *et al.* Myotube assembly on nanofibrous and micropatterned polymers. Nano Lett **6,** 537, 2006.
40. Yan, W., George, S., Fotadar, U., Tyhovych, N., Kamer, A., Yost, M.J., *et al.* Tissue engineering of skeletal muscle. Tissue Eng **13,** 2781, 2007.
41. Clark, P., Dunn, G.A., Knibbs, A., and Peckham, M. Alignment of myoblasts on ultrafine gratings inhibits fusion *in vitro*. Int J Biochem Cell Biol **34,** 816, 2002.
42. Lu, X., and Leng, Y. Comparison of the osteoblast and myoblast behavior on hydroxyapatite microgrooves. J Biomed Mater Res Part B Appl Biomater **90B,** 438, 2009.
43. Shimizu, K., Fujita, H., and Nagamori, E. Alignment of skeletal muscle myoblasts and myotubes using linear micropatterned surfaces ground with abrasives. Biotechnol Bioeng **103,** 631, 2009.
44. Altomare, L., Gadegaard, N., Visai, L., Tanzi, M.C., and Fare, S. Biodegradable microgrooved polymeric surfaces obtained by photolithography for skeletal muscle cell orientation and myotube development. Acta Biomater **6,** 1948, 2010.
45. Evans, D.J.R., Britland, S., and Wigmore, P.M. Differential response of fetal and neonatal myoblasts to topographical guidance cues *in vitro*. Dev Genes Evol **209,** 438, 1999.
46. Griffin, M.A., Sen, S., Sweeney, H.L., and Discher, D.E. Adhesion-contractile balance in myocyte differentiation. J Cell Sci **117,** 5855, 2004.
47. Mhanna, R.F., Voros, J., and Zenobi-Wong, M. Layer-by-layer films made from extracellular matrix macromolecules on silicone substrates. Biomacromolecules **12,** 609, 2011.
48. Peckham, M. Engineering a multi-nucleated myotube, the role of the actin cytoskeleton. J Microsc **231,** 486, 2008.
49. Horsley, V., and Pavlath, G.K. Forming a multinucleated cell: molecules that regulate myoblast fusion. Cells Tissues Organs **176,** 67, 2004.
50. Jaalouk, D.E., and Lammerding, J. Mechanotransduction gone awry. Nat Rev Mol Cell Biol **10,** 63, 2009.
51. Zhang, Q.P., Bethmann, C., Worth, N.F., Davies, J.D., Wasner, C., Feuer, A., *et al.* Nesprin-1 and −2 are involved in the pathogenesis of Emery-Dreifuss muscular dystrophy and are critical for nuclear envelope integrity. Hum Mol Genet **16,** 2816, 2007.

52. Zhang, J.L., Felder, A., Liu, Y.J., Guo, L.T., Lange, S., Dalton, N.D., *et al.* Nesprin 1 is critical for nuclear positioning and anchorage. Hum Mol Genet **19,** 329, 2010.
53. Brosig, M., Ferralli, J., Gelman, L., Chiquet, M., and Chiquet-Ehrismann, R. Interfering with the connection between the nucleus and the cytoskeleton affects nuclear rotation, mechanotransduction and myogenesis. Int J Biochem Cell Biol **42,** 1717, 2010.
54. Engel, A., and Franzini-Armstrong, C. Myology: Basic and Clinical. ed. New York: McGraw-Hill. Medical Pub. Division, 2004.
55. Levenberg, S., Rouwkema, J., Macdonald, M., Garfein, E.S., Kohane, D.S., Darland, D.C., *et al.* Engineering vascularized skeletal muscle tissue. Nat Biotechnol **23,** 879, 2005.
56. Koffler, J., Kaufman-Francis, K., Yulia, S., Dana, E., Daria, A.P., Landesberg, A., *et al.* Improved vascular organization enhances functional integration of engineered skeletal muscle grafts. Proc Natl Acad Sci U S A **108,** 14789, 2011.
57. Crouzier, T., Ren, K., Nicolas, C., Roy, C., and Picart, C. Layer-by-layer films as a biomimetic reservoir for rhBMP-2 delivery: controlled differentiation of myoblasts to osteoblasts. Small **5,** 598, 2009.
58. Picart, C., Elkaim, R., Richert, L., Audoin, T., Arntz, Y., Cardoso, M.D., *et al.* Primary cell adhesion on RGD-functionalized and covalently crosslinked thin polyelectrolyte multilayer films. Adv Funct Mater **15,** 83, 2005.
59. Mertz, D., Vogt, C., Hemmerle, J., Mutterer, J., Ball, V., Voegel, J.C., *et al.* Mechanotransductive surfaces for reversible biocatalysis activation. Nat Mater **8,** 731, 2009.

Address correspondence to:
Catherine Picart, Ph.D.
LMGP, CNRS UMR 5628 (LMGP)
Grenoble Institute of Technology and CNRS
3 parvis Louis Néel
F-38016 Grenoble Cedex
France

E-mail: catherine.picart@grenoble-inp.fr

Received: February 9, 2012
Accepted: April 3, 2012
Online Publication Date: July 5, 2012